

# Early type stars as calibrators for ground-based interferometry

Jinmi Yoon<sup>a</sup>, Deane M. Peterson<sup>a</sup>, Thomas Armstrong<sup>b</sup>, James H. Clark III<sup>c</sup>, Charmaine Gilbreath<sup>b</sup>, Thomas Pauls<sup>b</sup>, and Henrique R. Schmitt<sup>b</sup>

<sup>a</sup>Department of Physics and Astronomy, Stony Brook University, Stony Brook, NY 11794-3800 USA;

<sup>b</sup>Naval Research Laboratory, Code 7215, 4555 Overlook Avenue SW, Washington, DC, USA 20375;

<sup>c</sup>U.S. Naval Observatory, Flagstaff Station, P.O. Box 1149, Flagstaff, AZ 86002-1149, USA

## ABSTRACT

Visibility measurements with Michelson interferometers, particularly the measurement of fringe contrast, are affected by various atmospheric and instrumental effects, all of which reduce the measured contrast. To compensate for this, stars with known or predictable diameters (calibrators) are observed so that the overall reduction in the visibility can be measured. Objects with the smallest possible diameters are preferred as calibrators, since the predicted visibilities become less sensitive to any uncertainties. Therefore, unreddened, early type stars are usually chosen if they are available because they are relatively bright for a given angular diameter. However, early type stars bring additional complications. Rapid rotation, common with these stars can cause variations in the visibility amplitudes due to oblateness and surface brightness asymmetries that are larger than implied by the usual error estimates. In addition, rotation can introduce significant phase offsets. Using Roche models, von Zeipel theory, and the observed constraints of V, B-V, and  $v \sin i$ , it is possible to put limits on the size of these effects and even estimate the distribution of possible visibilities. To make this easily available to the community, we are in the process of creating a catalog of possible calibrators, including histograms of the visibilities, calculated for configurations used at a number of observatories. We show the examples of several early type stars which are potential calibrators using parameters appropriate for the Navy Prototype Optical Interferometer.

**Keywords:** Calibrators, Interferometry, Early type stars

## 1. INTRODUCTION

Michelson interferometers in principle measure the complex visibility, which is the Fourier transform of the object's surface brightness integrated perpendicular to the projected direction of the baseline<sup>1</sup>. However, the usual interferometric observables are the squared visibility amplitude, an unbiased estimator<sup>2</sup> and, if three or more apertures are available, the closure phase, which is free of atmospheric effects.

Various instrumental and atmospheric effects act to reduce the measured visibility amplitude and can add offsets to the phases. These can be corrected by observations of calibrators<sup>3</sup>. The squared visibility amplitude,  $V^2$ , of a science target is then obtained as

$$V^2 = \frac{\mu^2}{\mu_{cal}^2} V_{cal}^2, \quad (1)$$

where  $\mu$  and  $\mu_{cal}$  are the measured coherence factors of the target and the calibrator respectively, and the  $V_{cal}^2$  is the squared visibility amplitude of the calibrator, for which only estimates are usually available. Phases can be similarly adjusted, usually by additive corrections.

---

E-mail: jyoona@grad.physics.sunysb.edu, dpeterson@astro.sunysb.edu, tarmstr@nrl.navy.mil, jhc@sexton.lowell.edu, gilbreath@nrl.navy.mil, pauls@nrl.navy.mil, henrique.schmitt@nrl.navy.mil

Report Documentation Page				Form Approved OMB No. 0704-0188	
Public reporting burden for the collection of information is estimated to average 1 hour per response, including the time for reviewing instructions, searching existing data sources, gathering and maintaining the data needed, and completing and reviewing the collection of information. Send comments regarding this burden estimate or any other aspect of this collection of information, including suggestions for reducing this burden, to Washington Headquarters Services, Directorate for Information Operations and Reports, 1215 Jefferson Davis Highway, Suite 1204, Arlington VA 22202-4302. Respondents should be aware that notwithstanding any other provision of law, no person shall be subject to a penalty for failing to comply with a collection of information if it does not display a currently valid OMB control number.					
1. REPORT DATE <b>2006</b>		2. REPORT TYPE		3. DATES COVERED <b>00-00-2006 to 00-00-2006</b>	
4. TITLE AND SUBTITLE <b>Early type stars as calibrators for ground-based interferometry</b>				5a. CONTRACT NUMBER	
				5b. GRANT NUMBER	
				5c. PROGRAM ELEMENT NUMBER	
6. AUTHOR(S)				5d. PROJECT NUMBER	
				5e. TASK NUMBER	
				5f. WORK UNIT NUMBER	
7. PERFORMING ORGANIZATION NAME(S) AND ADDRESS(ES) <b>Naval Research Laboratory, Code 7215, 4555 Overlook Avenue SW, Washington, DC, 20375</b>				8. PERFORMING ORGANIZATION REPORT NUMBER	
9. SPONSORING/MONITORING AGENCY NAME(S) AND ADDRESS(ES)				10. SPONSOR/MONITOR'S ACRONYM(S)	
				11. SPONSOR/MONITOR'S REPORT NUMBER(S)	
12. DISTRIBUTION/AVAILABILITY STATEMENT <b>Approved for public release; distribution unlimited</b>					
13. SUPPLEMENTARY NOTES					
14. ABSTRACT <b>Visibility measurements with Michelson interferometers, particularly the measurement of fringe contrast, are affected by various atmospheric and instrumental effects, all of which reduce the measured contrast. To compensate for this, stars with known or predictable diameters (calibrators) are observed so that the overall reduction in the visibility can be measured. Objects with the smallest possible diameters are preferred as calibrators, since the predicted visibilities become less sensitive to any uncertainties. Therefore, unreddened, early type stars are usually chosen if they are available because they are relatively bright for a given angular diameter. However early type stars bring additional complications. Rapid rotation, common with these stars can cause variations in the visibility amplitudes due to oblateness and surface brightness asymmetries that are larger than implied by the usual error estimates. In addition, rotation can introduce significant phase offsets. Using Roche models, von Zeipel theory, and the observed constraints of V, B-V, and <math>v \sin i</math>, it is possible to put limits on the size of these effects and even estimate the distribution of possible visibilities. To make this easily available to the community, we are in the process of creating a catalog of possible calibrators, including histograms of the visibilities, calculated for configurations used at a number of observatories. We show the examples of several early type stars which are potential calibrators using parameters appropriate for the Navy Prototype Optical Interferometer.</b>					
15. SUBJECT TERMS					
16. SECURITY CLASSIFICATION OF:			17. LIMITATION OF ABSTRACT <b>Same as Report (SAR)</b>	18. NUMBER OF PAGES <b>7</b>	19a. NAME OF RESPONSIBLE PERSON
a. REPORT <b>unclassified</b>	b. ABSTRACT <b>unclassified</b>	c. THIS PAGE <b>unclassified</b>			

Stars having the smallest possible diameters are generally chosen as calibrators since the predicted visibilities are near maximum and hence less sensitive to uncertainties in the assumed diameters, which are of the order of a few percent when estimated by surface brightness-angular diameter relations<sup>3,4</sup>. However, most stars hotter than F5 rotate rapidly and rotation can introduce significant oblateness and surface brightness asymmetry in the apparent disks<sup>5</sup> which in turn can cause variations in the inferred diameters in addition to what is implied by the usual error estimates. In addition, asymmetry can cause a significant triple phase signal.

Here, we investigate how rotation might affect the use of the B-F stars as calibrators. We estimate the magnitude of the rotation effects using von Zeipel theory<sup>5</sup> and the constraints by provided by measurements of the magnitude and color, V and B-V, the projected equatorial velocity,  $v \sin i$ , and the parallax,  $\pi$ . In the next section we describe the gravity and limb-darkened Roche spheroid model of a calibrator. We introduce the instrumental parameters and the criteria for selecting B-F stars as calibrators in section 3. Then we describe the calculation of the simulations in section 4. Lastly, we describe the catalog of the calibrators we will produce.

## 2. A MODEL FOR EARLY TYPE STARS AS CALIBRATORS

The theory of rotating stars was studied by von Zeipel<sup>5</sup> in 1924. He showed that a rotating star adopts the figure of a Roche spheroid whose effective temperature is proportional to the fourth power of the effective gravity ( $T_{eff} \propto (g_{eff})^{\frac{1}{4}}$ ) under the assumptions of radiative equilibrium and solid body rotation. This theory has been tested not only in close binary systems but also through interferometric observations of isolated stars<sup>6-8</sup>. When calculating observables with this model, it is assumed that plane-parallel atmosphere describes the atmosphere locally. We use the ATLAS<sup>9</sup> models parametrized by Van Hamme<sup>10</sup>. Since these are hot stars we have adopted the square root parameterization of limb-darkening<sup>11</sup>.

## 3. SELECTION OF CALIBRATORS

### 3.1. Instrumental Parameters

Whether rotation introduces important asymmetries depends critically on combination of the wavelengths and baselines used. We focus here on the Navy Prototype Optical Interferometer<sup>12</sup> (NPOI) which has baselines up to 80 m. We adopt 500 nm as the nominal wavelength for calculating the squared visibilities.

### 3.2. Selection of Calibrators

**Table 1.** Examples of potential calibrators :  $v \sin i$  is in units of km/s. Angular diameter,  $\theta_{BEM}$  and parallax,  $\pi$  are in mas. The angular diameter was calculated using the Barnes-Evans-Moffet relation<sup>4</sup>.

HR	Name	RA	DEC	SpType	V	B-V	$v \sin i$	$\theta_{BEM}$	$\pi$
1673	68 Eri	050843.6	-042722	F2V	5.12	0.44	10	0.606	39.99
3974	21 LMi	100725.8	+351441	A7V	4.48	0.18	148	0.546	35.78
4733	14 Com	122624.1	+271606	F0p	4.95	0.27	227	0.505	11.92
8351	51 $\mu$ Cap	215317.8	-133306	F1III	5.08	0.37	87	0.554	36.15

Our input list of potential calibrators satisfies the following criteria: (1) luminosity class III, IV, and V stars in the color range  $B-V \leq 0.45$  as listed in the Bright Star Catalogue<sup>13</sup>, (2) declinations above  $-15^\circ$ , (3) angular size ( $\theta_{BEM}$ ) estimated using the Barnes-Evans-Moffet<sup>4</sup> relation between 0.5 mas and 1.5 mas, and (4) distance closer than 100 pc. The last eliminates significant reddening. We then pruned the list of any stars with companions with separations,  $\rho \leq 1''$  and magnitude differences,  $\Delta m < 5.0$ . However, unless second spectra were reported, we retained those listed or suspected as spectroscopic binaries. Examples of potential calibrators are shown in Table 1.

**Table 2.** The maximum, minimum, weighted average,  $\pm\sigma$  values of  $V^2$  of the sample stars with NPOI

HR	Name	$V_{max}^2$	$V_{min}^2$	$\overline{V^2}$	$-\sigma$	$+\sigma$
1673	68 Eri	0.656	0.629	0.630	0.629	0.630
3974	21 LMi	0.688	0.677	0.683	0.678	0.687
4733	14 Com	0.743	0.607	0.656	0.644	0.671
8351	51 $\mu$ Cap	0.701	0.678	0.683	0.680	0.686

## 4. SIMULATIONS AND CALCULATIONS

### 4.1. Procedure of Simulations

Roche models require several parameters. The initial inputs are inclination angle,  $i$ , mass, angular size,  $\theta$  (or equivalently the radius,  $R$ , through the parallax,  $\pi$ ), effective temperature,  $T_{eff}$ , and the dimensionless angular velocity,  $\omega$  ( $= \Omega/\Omega_B$  where  $\Omega$  is the angular velocity and  $\Omega_B$  is the angular velocity at break-up). We obtain a mass by finding the model in the Padova grid which reproduces the luminosity and polar radius.<sup>14</sup> During a simulation, the model is required to satisfy to the observed V, B-V and  $v \sin i$ . That is, we iterate until we match the projected rotational velocity ( $v \sin i$ ) by varying the angular velocity parameter ( $\omega$ ) or inclination angle ( $i$ ), or both. In the process the program must also iterate for consistent values of the polar values,  $T_{eff,p}$  and  $\theta_p$ , to match V magnitude and B-V, respectively. The models then allow us to predict visibilities as a function of the assumed Position Angle of the rotational axis.

In the process of these simulations we have found that calculated polar gravity,  $\log g_p$ , increases monotonically as the inclination angle decreases. The result is that for many candidates the potential range of the inclinations is terminated well before reaching break-up angular velocity ( $\omega = 0.999$ ) because the predicted gravities would exceed those of the predicted Zero Age Main Sequence (ZAMS).

Squared visibilities can be calculated at any inclination angle and a Position Angle allowed by the mentioned constraints of the observed quantities. The allowed inclination angles are between  $i = 90^\circ$  and the "critical angle" if limited by ZAMS constraints on the gravity. However, if there are no restrictions of the gravity, we do simulations up to the break-up angle. The squared visibilities are sampled at 12 evenly spaced Position Angles and 20 evenly spaced inclinations in the allowed range of each star.

### 4.2. Statistical Calculations

Using the visibilities calculated over the range of inclinations and Position Angles, we generate the histograms describing the probability distribution, and calculate the maximum, minimum, average, and 95% confidence levels of  $V^2$ . The only assumption here is that the rotational axis is randomly oriented<sup>15</sup> over the range of allowed inclinations and Position Angles.

The histograms are constructed by dividing the range of squared visibilities into ten bins. The probability,  $P_k$  of squared visibilities being the  $k$ th bin is then given by,

$$P_k = P(V_k^2 \leq V^2 < V_{k+1}^2) = \frac{\sum_l^{n_k} \sin i_l}{\sum_j^N \sin i_j}, \quad (2)$$

$$P = \sum_{k=1}^{10} P_k = 1, \quad (3)$$

where  $N$  and  $n_k$  are the total number of inclination and position angle samples and the number that satisfy  $V_k^2 \leq V^2 < V_{k+1}^2$  respectively. And  $i_j$  and  $i_l$  are the inclination angles at the sample points.

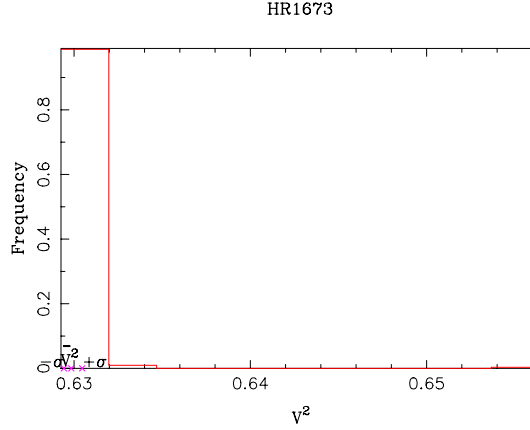


**Figure 1.** The histogram for HR 1673: This star is a slow rotator with  $v \sin i = 10 \text{ km/s}$ . In spite of its slow rotation and a narrow range of  $\pm\sigma$  the histogram displays an extended tail, albeit of low probability. These extreme visibilities result from the fact that star could be seen nearly pole on. The star should be used as a calibrator with some caution.

The weighted average of the squared visibilities,  $\overline{V^2}$ , of the star, corresponding to the inclination angles, is obtained from

$$\overline{V^2} = \frac{\sum_j^N V_j^2 \sin i_j}{\sum_j^N \sin i_j}, \quad (4)$$

where  $V_j^2$  is the squared visibility at the  $j$ th sample. Finally, we tabulate squared visibilities of the 95 % level of significance, indicated as " $\pm\sigma$ ", as well as the maximum ( $V_{max}^2$ ) and minimum ( $V_{min}^2$ ) values.

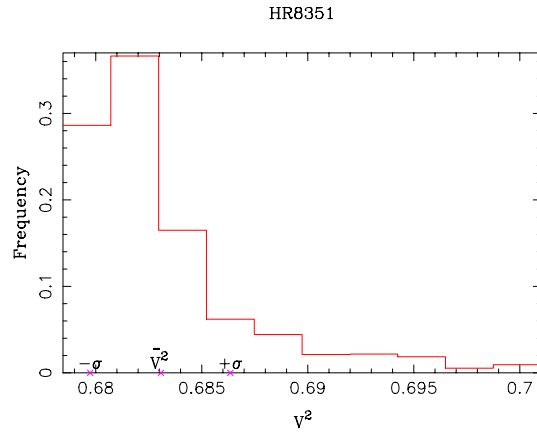
## 5. RESULTS

We limit our discussion here to visibility amplitudes. Estimates in inferred angular diameters by the surface brightness-angular diameter relations are uncertain by a few percent. Adopting the 3% uncertainty suggested by Muzurkwich et al.<sup>3</sup> in a star with a uniform disk angular diameter of  $\theta=0.55 \text{ mas}$ , measured with a 80 m baseline at 550 nm experiences an uncertainty in  $V^2 = 0.63$  of about 0.02. The effects of rotation on the visibilities can be substantially larger than this.

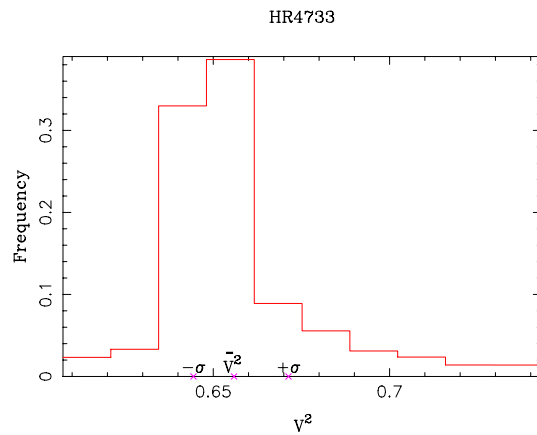
To illustrate the range of results, we consider 4 cases listed in Table 1. They include a slow rotator (HR 1673), an intermediate rotator (HR 8351), and two moderately fast rotators (HR 3974, HR 4733). Note that by usual standards all would at first glance be good calibrator choices, with angular diameters nominally in the range 0.5-0.6 mas.

Table 2 presents the results of the simulations where  $V_{min}^2$ ,  $V_{max}^2$ ,  $\overline{V^2}$ , and  $\pm\sigma$  values of the squared visibilities of each star are given. The histograms derived from these calculations are shown in Fig 1 through Fig 4 which show the probability distribution of the  $V^2$  values according to the allowed range of inclinations and Position Angles. The bin size for the histograms is a tenth of the range  $V_{max}^2$  to  $V_{min}^2$  if this is larger than 0.2 percent of  $\overline{V^2}$ , and otherwise fixed at 0.2% of the average if the range is less than 2% of  $\overline{V^2}$ .

Stars with small projected rotational velocities, predicted to be or near the ZAMS such as will show no significant variation in their visibilities. These are ideal calibrators and we have identified a number in our catalog. On the other hand, the slow rotator, HR 1673, illustrated in Fig 1, shows an extended, low probability tail in the squared visibility. Even though it is likely to have the nominal visibility, there is a finite chance of a 4 % error. In the simulations for this star the inclination was cut off at an inclination of  $i = 2.45^\circ$ , with smaller



**Figure 2.** The histogram for HR 8351: This star is an intermediate rotator with  $v \sin i = 87$  km/s. The histogram shows the rotational effects on its visibility. This star can be a calibrator, but the variation of squared visibilities should be properly considered because of the extended tail of possible  $V^2$  values. The abscissa covers the entire range of visibilities.



**Figure 3.** The histogram for HR 4733: This star is a fast rotator with  $v \sin i = 227$  km/s. As expected, the rotation significantly affects the visibilities. This is an example of a star with a small predicted angular diameter, 0.505 mas, which could nevertheless produce significant calibration errors.

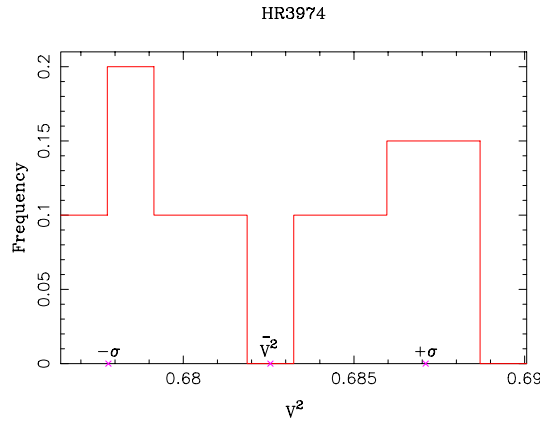


**Figure 4.** The histogram for HR 3974 : This is a moderately rotating star with  $v \sin i = 148$  km/s which is on or very near the ZAMS. This can be a good calibrator because of the small predicted range in  $V^2$ . However, it is clear that its rotation does produce some uncertainty in its visibility. Here, the size of bin is the 0.2 percent of  $\overline{V^2}$ .

inclinations pushing the models below the ZAMS. Even with critical rotation excluded, the high inclination that are accessible can generate significant uncertainties in the visibilities.

Fig 2 shows the histogram of squared visibilities for HR 8351, which has an intermediate projected rotational velocity of 87 km/s. This rotation can result in significant range of visibilities for this star. Although a reasonable candidate as a calibrator as with HR 1631, this star can add uncertainty to visibility measurements.

For the moderately fast rotator HR 4733 we show how its rotation affects the predicted squared visibilities in Fig 3. Significant flattening is predicted at all inclinations, so the visibility measurements vary significantly over the possible combinations of inclinations and position angles. In spite of a small predicted angular diameter, 0.505 mas, the range in the visibilities must be considered calibrating with this star.

In Fig 4, we show the visibility range for HR 3974, a star with moderately fast projected rotation. HR 3974 appear to lie on or very the ZAMS which greatly limits the predicted range of visibilities, allowing it to be a good calibrator in spite of its significant projected velocity. The double horned shape of the resulting histogram is characteristic of stars near the ZAMS affected by significant rotation.

By looking through the variety of histograms, one can identify the kinds of early type stars that can be good calibrators. The expected cases, early type stars with small angular diameter and small projected rotational velocities are not guaranteed to be good calibrators. However, stars that can be identified as on or near the ZAMS are generally good calibrators because of their narrow visibility distribution even with significant rotation.

## 6. CONCLUSIONS

We are preparing a catalog of early type stars (unreddened and hot stars) with small diameters that can serve as calibrators. Generally, for these stars the predicted visibilities are less sensitive to uncertainties in the predicted diameters and they are relatively bright at a given angular size. However fast rotation, common with these stars, causes variations in the inferred visibilities due to oblateness which might be larger than implied by the errors estimated for the angular diameters. Using Roche models, von Zeipel theory, and the observed constraints of  $V$ ,  $B-V$ , and  $v \sin i$ , we estimated the range in visibilities that might be induced by rotation. Visibility histograms of some representative examples illustrate the effects of rotation and proximity to the ZAMS. Early type stars with small diameter not affected by fast rotation are not guaranteed to be good calibrators. We have also found that stars on or near ZAMS can also be reliable calibrators, even with moderate projected rotational velocities.

## ACKNOWLEDGMENTS

J. Y. is supported by a grant from the Naval Research Laboratory to D. M. P.

## REFERENCES

1. P. Hariharan, *Optical interferometry*, Elsevier, 2003.
2. M. M. Colavita, "Fringe visibility estimators for the Palomar Testbed Interferometer," *PASP* **111**, 1999.
3. D. Muzurchwich et al., "Angular diameters of stars from the Mark III Optical interferometer," *ApJ* **126**, 2003.
4. T. G. Barnes, D. S. Evans, and T. J. Moffet, "Stellar angular diameters and visual surface brightness - III. An improved definition of the relationship," *Mon. Not. R. Astro. Soc.* **183**, pp. 285–304, 1978.
5. H. von Zeipel, "The radiative equilibrium of a slightly oblate rotating star," *Mon. Not. R. Astro. Soc.* **84**, pp. 684–701, 1924.
6. D. M. Peterson et al., "Resolving the effects of rotation in altair with long-baseline interferometry," *ApJ* **636**, pp. 1087–1097, 2006.
7. D. M. Peterson et al., "Vega is a rapid rotating star," *Nature* **440**, pp. 896–899, 2006.
8. A. Domiciano de Souza et al., "Gravitational-darkening of altair from interferometry," *A & Ap* **442**, pp. 567–578, 2005.
9. R. L. Kurucz, *Cd-rom no.13*, Smithsonian Astrophysical Observatory, 1993.
10. W. V. Hamme, "New limb-darkening coefficients for modeling binary light curves," *AJ* **106**, pp. 2069–2117, 1993.
11. J. Díaz-Cordovés and A. Giménez, "A new nonlinear approximation to the limb-darkening of hot stars," *A. & Ap.* **259**, pp. 227–231, 1992.
12. J. T. Armstrong et al., "The Navy Prototype Optical Interferometer," *ApJ* **496**, pp. 550–571, 1998.
13. D. Hoffleit and W. H. Warren Jr, *Bright Star Catalogue*, 2005(5th Revised edition). <http://cdsweb.u-strasbg.fr/cgi-bin/Cat?V/50>.
14. L. Girardi, A. Bressan, G. Bertelli, and C. Chiosi, "Evolutionary tracks and isochrones for low- and intermediate-mass stars: From 0.15 to 7  $M_{sun}$ , and from  $z=0.0004$  to 0.03," *ApJS* **141**, pp. 371–383, 2000.
15. A. J. Deutsch, "Maxwellian distributions for stellar rotations," in *Stellar Rotation*, pp. 207–218, Gordon and Breach (first edition), New York, 1969.